

Learning Student-Friendly Teacher Networks for Knowledge Distillation

Dae Young Park^{*1} Moon-Hyun Cha¹ Changwook Jeong¹ Daesin Kim¹ Bohyung Han^{*2}

Abstract

We propose a novel knowledge distillation approach to facilitate the transfer of dark knowledge from a teacher to a student. Contrary to most of the existing methods that rely on effective training of student models given pretrained teachers, we aim to learn the teacher models that are friendly to students and, consequently, more appropriate for knowledge transfer. In other words, even at the time of optimizing a teacher model, the proposed algorithm learns the student branches jointly to obtain student-friendly representations. Since the main goal of our approach lies in training teacher models and the subsequent knowledge distillation procedure is straightforward, most of the existing knowledge distillation algorithms can adopt this technique to improve the performance of the student models in terms of accuracy and convergence speed. The proposed algorithm demonstrates outstanding accuracy in several well-known knowledge distillation techniques with various combinations of teacher and student architectures.

1. Introduction

Knowledge distillation (Hinton et al., 2015) is a well-known technique to learn compact deep neural network models with competitive accuracy, where a smaller network (student) is trained to simulate the representations of a larger one (teacher) with higher accuracy. The popularity of knowledge distillation is mainly due to its simplicity and generality; it is straightforward to learn a student model based on a teacher and there is no restriction about the network architectures of both models. The main goal of most approaches is how to transfer dark knowledge to student models effectively, given predefined or pretrained teacher networks.

Although knowledge distillation is a promising and convenient method, it sometimes fails to achieve satisfactory performance in terms of accuracy. This is partly because

the model capacity of student is too limited compared to that of teacher and knowledge distillation algorithms are suboptimal (Kang et al., 2020; Mirzadeh et al., 2020). In addition to this reason, we claim that the consistency of teacher and student features is critical to knowledge transfer and the inappropriate representation learning of a teacher often leads to suboptimality of knowledge distillation.

We are interested in making a teacher network hold better transferable knowledge by providing the teacher with a snapshot of the student model at the time of its training. We employ the typical structures of convolutional neural networks based on multiple blocks and make the representations of each block in the teacher easy to be transferred to the student. The proposed approach aims to train teacher models friendly to students for facilitating knowledge distillation; we call the teacher model trained by this strategy student-friendly teacher network (SFTN). SFTN is deployed in arbitrary distillation algorithms easily due to its generality for training models and transferring knowledge.

SFTN is somewhat related to collaborative learning methods (Zhang et al., 2018b; Guo et al., 2020; Wu & Gong, 2020), but does perform knowledge transfer from teacher to student in one direction. More importantly, the models given by collaborative learning are prone to be correlated and may not be appropriate for fully exploiting knowledge in teacher models. On the other hand, SFTN adopts a two-stage learning procedure to alleviate the limitation: student-aware training of teacher network followed by knowledge distillation from teacher to student. Figure 1 demonstrates the main difference between the proposed algorithm and the standard knowledge distillation methods.

The following is the list of our main contributions:

- We adopt a student-aware teacher learning procedure before knowledge distillation, which enables teacher models to transfer their representations to students more effectively.
- The proposed approach is applicable to diverse architectures of teacher and students while it can be incorporated into various knowledge distillation algorithms.
- We illustrate that the integration of SFTN into various baseline algorithms and models improve accuracy

^{*}Equal contribution ¹DIT Center, Samsung Electronics, Korea ²Seoul National University, Korea. Correspondence to: Dae Young Park <p30.daeyoung@samsung.com>, Bohyung Han <bhan@snu.ac.kr>.

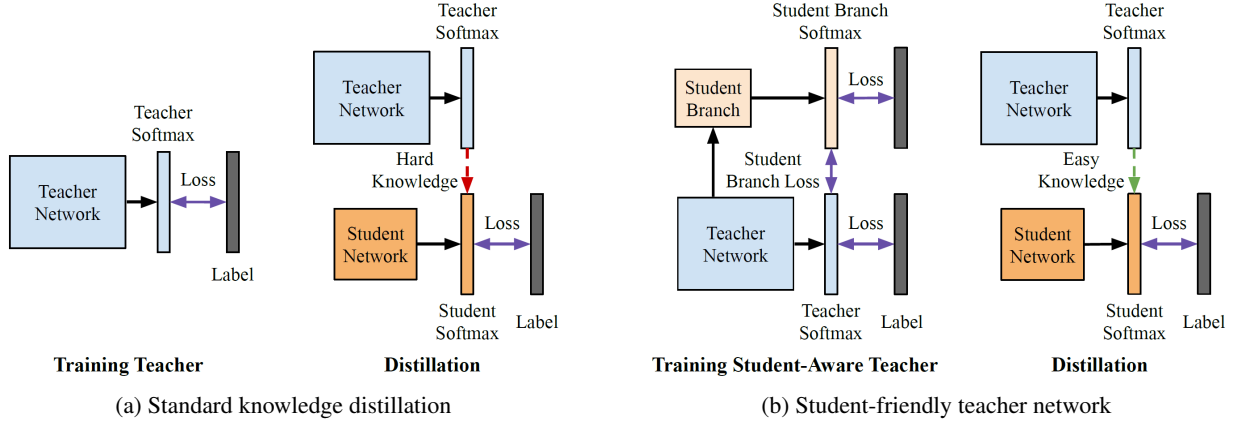


Figure 1. Comparison between the standard knowledge distillation and our approach. (a) The standard knowledge distillation trains teachers alone and then distill knowledge to students. (b) The proposed student-friendly teacher network trains teachers along with student branches, and then distill more easy-to-transfer knowledge to students.

consistently with substantial margins.

The rest of the paper is organized as follows. We first discuss the existing knowledge distillation techniques in Section 2. Section 3 describes the details of the proposed SFTN including the knowledge distillation algorithm. The experimental results with in-depth analysis are presented in Section 4, and we make the conclusion in Section 5.

2. Related Work

Although deep learning has shown successful outcomes in various areas, it is still difficult to apply deep neural networks to real-world problems due to the constraints of computation and memory resources. There have been many attempts to reduce the computational cost of deep learning models, and knowledge distillation is one of the examples. Various computer vision (Chen et al., 2017; Luo et al., 2016; Wu et al., 2019; Wang et al., 2020) and natural language processing (Jiao et al., 2019; Mun et al., 2018; Sanh et al., 2019; Arora et al., 2019) tasks often employ knowledge distillation to obtain efficient models. Recently, some cross-modal tasks (Thoker & Gall, 2019; Zhao et al., 2018; Zhou et al., 2020) adopt it to transfer knowledge across domains. This section summarizes the research efforts to the performance of models via knowledge distillation.

2.1. What to distill

Since Hinton et al. (Hinton et al., 2015) introduces the basic concept of knowledge distillation, where the knowledge is given by the temperature-scaled representations of the softmax function in teacher models, various kinds of information have been employed as the sources of knowledge for distillation from teachers to students. FitNets (Romero et al., 2015) distills intermediate features of a teacher network, where the student network transforms the intermediate fea-

tures using guided layers and then calculates the difference between the guided layers and the intermediate features of teacher network. The position of distillation to the layer is shifted to the layers before ReLU operations in (Heo et al., 2019a), which also proposes the novel activation function and the partial L_2 loss function for effective knowledge transfer. Zagoruyko and Nikos Komodakis (Zagoruyko & Komodakis, 2017) argue importance of attention and proposes an attention transfer (AT) method from teachers to students while Kim et al. (Kim et al., 2018) compute the factor information of the teacher representations using autoencoder, which is decoded by students for knowledge transfer. Relational knowledge distillation (RKD) (Park et al., 2019) introduces a technique to transfer relational information such as distances and angles of features.

CRD (Tian et al., 2020) maximizes mutual information between student and teacher via contrastive learning while ONE (lan et al., 2018) and BYOT (Zhang et al., 2019) transfer knowledge without teacher. There exist a couple of methods to perform knowledge distillation without teacher models. For example, (lan et al., 2018) distills knowledge from an ensemble of multiple students, and BYOT (Zhang et al., 2019) transfers knowledge from deeper layers to shallower ones. Besides, SSKD (Xu et al., 2020) distills self-supervised features of teachers to students for transferring richer knowledge.

2.2. How to distill

Several recent knowledge distillation methods focus on the strategy of knowledge distillation. Born again network (BAN) (Furlanello et al., 2018) presents the effectiveness of sequential knowledge distillation via the networks with an identical architecture. A curriculum learning method (Jin et al., 2019) employs the optimization trajectory of a teacher model to train students. Collaborative

learning approaches (Zhang et al., 2018b; Guo et al., 2020; Wu & Gong, 2020) attempt to learn multiple models with distillation jointly, but their concept is not well-suited for asymmetric teacher-student relationship, which may lead to suboptimal convergence of student models.

The model capacity gap between a teacher and a student is addressed in (Kang et al., 2020; Cho & Hariharan, 2019; Mirzadeh et al., 2020). TAKD (Mirzadeh et al., 2020) suggests the teacher assistant network to reduce model capacity gap, where a teacher model transfer knowledge to student via a teaching assistant with an intermediate size. An early stopping technique for training teacher networks is proposed to obtain better transferable representations and a neural architecture search is employed to identify a student model with the optimal size (Kang et al., 2020). Our work proposes a novel student-friendly learning technique of teacher networks to facilitate knowledge distillation.

3. Student-Friendly Knowledge Distillation

This section describes the details of the student-friendly teacher network (SFTN), which transfers the features of teacher models to student networks more effectively than the standard distillation. Figure 2 illustrates the main idea of our method.

3.1. Overview

The conventional knowledge distillation approaches attempt to find the way of teaching student networks given the architecture of teacher networks. Since the teacher network is trained only with the loss with respect to the ground-truth, and the optimization of the objective is not necessarily beneficial for knowledge distillation to students. To the contrary, SFTN framework aims to improve the effectiveness of knowledge distillation from the teacher to the student models. The procedure of SFTN is composed of the following steps.

Modularizing teacher and student networks We modularize teacher and student networks into multiple blocks based on the depth of layers and the feature map sizes. This is because knowledge distillation is often performed at every 3 or 4 blocks for accurate extraction and transfer of knowledge in teacher models. Figure 2 presents the case that both networks are modularized into 3 blocks, denoted by $\{B_T^1, B_T^2, B_T^3\}$ and $\{B_S^1, B_S^2, B_S^3\}$ for teacher and student, respectively.

Adding student branches SFTN adds student branches to a teacher model for joint training of both parts. Each student branch is composed of a teacher network feature transform layer \mathcal{T} and a student network blocks. Note that \mathcal{T} is similar to a guided layer in FitNets (Romero et al., 2015) and transforms the dimensionality of channel in F_T^i

into B_S^{i+1} . Depending on the configuration of teacher and student networks, the transformation need to increase or decrease the size of the feature maps. We employ 3×3 convolutions to reduce the size of F_T^i while 4×4 transposed convolutions are used to increase its size. Also, 1×1 convolutions is used when we do not need to change the size of F_T^i . The features transformed to a student branch is forwarded separately to compute the logit of the branch. For example, as shown in Figure 2(a), F_T^1 in the teacher stream is transformed to B_S^2 , which initiates a student branch to derive q_R^1 while another student branch starts from the transformed features from F_T^2 . Note that F_T^3 has no trailing teacher network block in the figure and has no associated student branch.

Training SFTN The teacher network is trained along with multiple student branches corresponding to individual blocks in the teacher, where the loss is given by the differences in the representations between the teacher and the student branches. Our loss function is composed of three terms: loss in the teacher network \mathcal{L}_T , Kullback-Leibler loss \mathcal{L}_R^{KL} in the student branch, and cross-entropy loss \mathcal{L}_R^{CE} in the student branch. The main loss term, \mathcal{L}_T , minimizes the error between q_T and the ground-truth while \mathcal{L}_R^{KL} enforces q_R^i and q_T to be similar to each other and \mathcal{L}_R^{CE} makes q_R^i fit the ground-truth.

Distillation using SFTN As shown in Figure 2(b), the conventional knowledge distillation technique is employed to transfer F_T^i and q_T simulated by F_S^i and q_S respectively. The actual knowledge distillation step is straightforward because the representations of F_T^i and q_T have already been learned properly at the time of training SFTN. We expect the performance of the student network distilled from the SFTN to be better than the one obtained from the conventional teacher network.

3.2. Network Architecture

SFTN consists of a teacher network and multiple student branches. The teacher and student networks are divided into N blocks, where a set of blocks in the teacher is given by $\mathbb{B}_T = \{B_T^i\}_{i=1}^N$ while the blocks in the student is denoted by $\mathbb{B}_S = \{B_S^i\}_{i=1}^N$. Note that the last block in the teacher network does not have the associated student branch.

Let x be an input of the network. Then, the softmax function output of the teacher network, q_T , is given by

$$q_T = \text{softmax} \left(\frac{\mathcal{F}_T(x)}{\tau} \right), \quad (1)$$

where \mathcal{F}_T denotes the logit of the teacher network and τ is the parameter to determine the smoothness of the softmax function. On the other hand, the output of the softmax

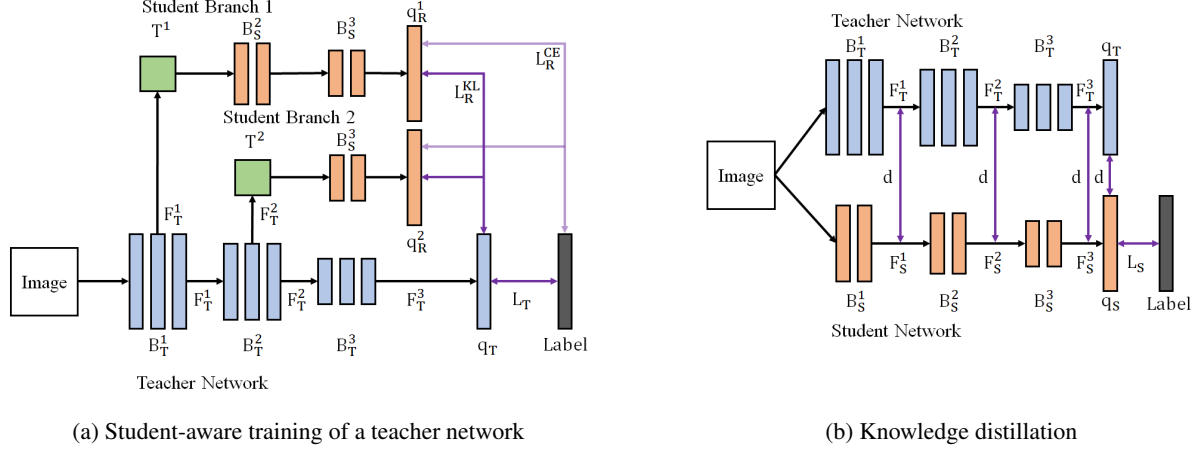


Figure 2. Overview of the student-friendly teacher network (SFTN). In this figure, \mathbf{F}_T^i , \mathbf{F}_S^i , B_T^i , B_S^i , \mathcal{T}^i , \mathbf{q}_R^i , \mathbf{q}_T , and \mathbf{q}_S denote the i^{th} teacher network feature, the i^{th} student network feature, the i^{th} block of teacher network, the i^{th} block of student network, teacher network feature transform layer, softmax output of the i^{th} student branch, softmax output of teacher network, and softmax output of student network, respectively. The loss for teacher network \mathcal{L}_T is given by Eqn. (4), Kullback-Leibler loss $\mathcal{L}_R^{\text{KL}}$ and cross entropy loss $\mathcal{L}_R^{\text{CE}}$ are defined in Eqn. (5) and Eqn. (6), respectively. (a) While training a teacher, SFTN trains \mathbf{F}_T^i and \mathbf{q}_T for better knowledge transfer to student networks. (b) In the distillation stage, the features in the teacher network, \mathbf{F}_T^i and \mathbf{q}_T , are distilled to student networks with existing knowledge distillation algorithms straightforwardly.

function in the i^{th} student branch, \mathbf{q}_R^i , is given by

$$\mathbf{q}_R^i = \text{softmax} \left(\frac{\mathcal{F}_S^i(\mathcal{T}^i(\mathbf{F}_T^i))}{\tau} \right), \quad (2)$$

where \mathcal{F}_S^i denotes the logit of the i^{th} student branch.

3.3. Loss Functions

The teacher network in the conventional knowledge distillation framework is trained only with \mathcal{L}_T . However, SFTN has additional loss terms such as $\mathcal{L}_R^{\text{KL}}$ and $\mathcal{L}_R^{\text{CE}}$ as described in Section 3.1. The total loss function of SFTN, denoted by $\mathcal{L}_{\text{SFTN}}$, is given by

$$\mathcal{L}_{\text{SFTN}} = \lambda_T \mathcal{L}_T + \lambda_R^{\text{KL}} \mathcal{L}_R^{\text{KL}} + \lambda_R^{\text{CE}} \mathcal{L}_R^{\text{CE}}, \quad (3)$$

where λ_T , λ_R^{KL} and λ_R^{CE} are the weights of individual loss terms.

Each loss term is defined as follows. First, \mathcal{L}_T is given by the cross-entropy between \mathbf{q}_T and the ground-truth label \mathbf{y} as

$$\mathcal{L}_T = \text{CrossEntropy}(\mathbf{q}_T, \mathbf{y}). \quad (4)$$

The knowledge distillation loss, $\mathcal{L}_R^{\text{KL}}$, employs the KL divergence between \mathbf{q}_R^i and \mathbf{q}_T , where $N - 1$ student branches except for the last block in the teacher network are considered together as

$$\mathcal{L}_R^{\text{KL}} = \frac{1}{N-1} \sum_{i=1}^{N-1} \text{KL}(\mathbf{q}_R^i || \mathbf{q}_T). \quad (5)$$

The cross-entropy loss of the student network, $\mathcal{L}_R^{\text{CE}}$, is obtained by the average cross-entropy loss from all the student

branches, which is given by

$$\mathcal{L}_R^{\text{CE}} = \frac{1}{N-1} \sum_{i=1}^{N-1} \text{CrossEntropy}(\mathbf{q}_R^i, \mathbf{y}). \quad (6)$$

3.4. Discussion

SFTN learns teacher models that transfer knowledge to students more effectively. One drawback of the proposed method is the increase of training cost due to the two-stage training framework. However, the main goal of knowledge distillation is to maximize the benefit in student networks, and the additional training cost may not be critical in many real applications. In the next section, we show that SFTN is effective to learn high-performance student models combined with various knowledge distillation techniques.

4. Experiments

We evaluate the performance of SFTN in comparison to existing methods and analyze the characteristics of SFTN in various aspects. We first describe our experiment setting in Section 4.1. Then, we compare results between SFTN and the standard teacher networks with respect to classification accuracy in various knowledge distillation algorithms in Section 4.2. The results from ablative experiments for SFTN and transfer learning are discussed in the rest of this section.

4.1. Experiment Setting

We perform evaluation on multiple well-known datasets including ImageNet (Russakovsky et al., 2015). CIFAR-

Table 1. Comparisons between SFTN and the standard teacher models on CIFAR-100 dataset when the architectures of the teacher-student pairs are homogeneous. In all the tested algorithms, the student models distilled from the teacher models given by SFTN outperform the ones trained from the standard teacher models. All the reported accuracies in this table is computed by the outputs of 3 independent runs.

Models (Teacher/Student) Teacher training method	WRN40-2/WRN16-2			WRN40-2/WRN40-1			resnet32x4/resnet8x4			resnet32x4/resnet8x2		
	Standard	SFTN	Δ	Standard	SFTN	Δ	Standard	SFTN	Δ	Standard	SFTN	Δ
Teacher Accuracy	76.30	78.20		76.30	77.62		79.25	79.41		79.25	77.89	
Student accuracy w/o KD		73.41			72.16			72.38			68.19	
KD	75.46	76.25	+0.79	73.73	75.09	+1.36	73.39	76.09	+2.70	67.43	69.17	+1.74
FitNets	75.72	76.73	+1.01	74.14	75.54	+1.40	75.34	76.89	+1.55	69.80	71.07	+1.27
AT	75.85	76.82	+0.97	74.56	75.86	+1.30	74.98	76.91	+1.93	68.79	70.90	+2.11
SP	75.43	76.77	+1.34	74.51	75.31	+0.80	74.06	76.37	+2.31	68.39	70.03	+1.64
VID	75.63	76.79	+1.16	74.21	75.76	+1.55	74.86	77.00	+2.14	69.53	71.08	+1.55
RKD	75.48	76.49	+1.01	73.86	75.11	+1.25	74.12	76.62	+2.50	68.54	70.91	+2.36
PKT	75.71	76.57	+0.86	74.43	75.49	+1.06	74.70	76.57	+1.87	69.29	70.75	+1.45
AB	70.12	70.76	+0.64	74.38	75.51	+1.13	74.73	76.51	+1.78	69.76	71.05	+1.29
FT	75.6	76.51	+0.91	74.49	75.11	+0.62	74.89	77.02	+2.13	69.70	71.11	+1.40
CRD	75.91	77.23	+1.32	74.93	76.09	+1.16	75.54	76.95	+1.41	70.34	71.34	+1.00
SSKD	75.96	76.80	+0.84	75.72	76.03	+0.31	75.95	76.85	+0.90	69.34	70.29	+0.96
OH	76.00	76.39	+0.39	74.79	75.62	+0.83	75.04	76.65	+1.61	68.10	69.69	+1.59
Best	76.00	77.23	+1.23	75.72	76.09	+0.37	75.95	77.02	+1.07	70.34	71.34	+1.00

Table 2. Comparisons between SFTN and the standard teacher models on CIFAR-100 dataset when the architectures of the teacher-student pairs are heterogeneous. In all the tested algorithms, the student models distilled from the teacher models given by SFTN outperform the ones trained from the standard teacher models. All the reported accuracies in this table is computed by the outputs of 3 independent runs.

Models (Teacher/Student) Teacher training method	resnet32x4/ShuffleV1			resnet32x4/ShuffleV2			ResNet50/VGG8			WRN40-2/ShuffleV2		
	Standard	SFTN	Δ	Standard	SFTN	Δ	Standard	SFTN	Δ	Standard	SFTN	Δ
Teacher Accuracy	79.25	80.03		79.25	79.58		78.70	82.52		76.30	78.21	
Student accuracy w/o KD		71.95			73.21			71.12			73.21	
KD	74.26	77.93	+3.67	75.25	78.07	+2.82	73.82	74.92	+1.10	76.68	78.06	+1.38
FitNets	75.95	78.75	+2.80	77.00	79.68	+2.68	73.22	74.80	+1.58	77.31	79.21	+1.90
AT	76.12	78.63	+2.51	76.57	78.79	+2.22	73.56	74.05	+0.49	77.41	78.29	+0.88
SP	75.80	78.36	+2.56	76.11	78.38	+2.27	74.02	75.37	+1.35	76.93	78.12	+1.19
VID	75.16	78.03	+2.87	75.70	78.49	+2.79	73.59	74.76	+1.17	77.27	78.78	+1.51
RKD	74.84	77.72	+2.88	75.48	77.77	+2.29	73.54	74.70	+1.16	76.69	78.11	+1.42
PKT	75.05	77.46	+2.41	75.79	78.28	+2.49	73.79	75.17	+1.38	76.86	78.28	+1.42
AB	75.95	78.53	+2.58	76.25	78.68	+2.43	73.72	74.77	+1.05	77.28	78.77	+1.49
FT	75.58	77.84	+2.26	76.42	78.37	+1.95	73.34	74.77	+1.43	76.80	77.65	+0.85
CRD	75.60	78.20	+2.60	76.35	78.43	+2.08	74.52	75.41	+0.89	77.52	78.81	+1.29
SSKD	78.05	79.10	+1.05	78.66	79.65	+0.99	76.03	76.95	+0.92	77.81	78.34	+0.53
OH	77.51	79.56	+2.05	78.08	79.98	+1.90	74.55	75.95	+1.40	77.82	79.14	+1.32
Best	78.05	79.56	+1.51	78.66	79.98	+1.32	76.03	76.95	+0.92	77.82	79.21	+1.39

100 (Krizhevsky, 2009), and STL10 (Coates et al., 2011). For the experiment, we select several different backbone networks such as ResNet (He et al., 2016), WideResNet (Zagoruyko & Komodakis, 2016), VGG (Simonyan & Zisserman, 2015), ShuffleNetV1 (Zhang et al., 2018a), and ShuffleNetV2 (Tan et al., 2019).

For comprehensive evaluation, we adopt various knowledge distillation techniques, which include KD (Hinton et al., 2015), FitNets (Romero et al., 2015), AT (Zagoruyko & Komodakis, 2017), SP (Tung & Mori, 2019), VID (Ahn et al., 2019), RKD (Park et al., 2019), PKT (Passalis & Tefas, 2018), AB (Heo et al., 2019b), FT (Kim et al., 2018), CRD (Tian et al., 2020), SSKD (Xu et al., 2020), and OH (Heo et al., 2019a). Among these methods, the feature distillation methods (Romero et al., 2015; Zagoruyko & Komodakis, 2017; Tung & Mori, 2019; Ahn et al., 2019;

Park et al., 2019; Passalis & Tefas, 2018; Heo et al., 2019b; Kim et al., 2018; Heo et al., 2019a) conduct joint distillation with conventional KD (Hinton et al., 2015) during student training, which results in higher accuracy in practice than the feature distillation only. We also include comparisons with collaborative learning methods such as DML (Zhang et al., 2018b) and KDCL (Guo et al., 2020), and a curriculum learning technique, RCO (Jin et al., 2019). We have reproduced the results from the existing methods using the implementations provided by the authors of the papers.

4.2. Main Results

To show effectiveness of SFTN, we incorporate SFTN into various existing knowledge distillation algorithms and evaluate accuracy. We present implementation details and experimental results on CIFAR-100 (Krizhevsky, 2009) and

ImageNet (Russakovsky et al., 2015) datasets.

4.2.1. CIFAR-100

CIFAR-100 (Krizhevsky, 2009) consists of 50K training images and 10K testing images in 100 classes. We select 12 state-of-the-art distillation methods to compare accuracy of SFTN with the standard teacher network. To show the generality of the proposed approach, 8 pairs of teacher and student models have been tested in our experiment. The experiment setup for CIFAR-100 is identical to the one performed in CRD¹; most experiments employ the SGD optimizer with learning rate 0.05, weight decay 0.0005 and momentum 0.9 while learning rate is set to 0.01 in ShuffleNet experiments. The hyper-parameters for the loss function are set as $\lambda_T = 1$, $\lambda_R^{CE} = 1$, $\lambda_R^{KL} = 3$, and $\tau = 1$.

Table 1 and 2 demonstrates the full results on the CIFAR-100 dataset. Table 1 presents distillation performance of all the compared algorithms when the architecture styles of teacher and student pairs are same while Table 2 shows distillation performance of teacher-student pairs with different architecture styles. Both tables clearly present that SFTN is consistently better than the standard teacher network in all experiments. The average difference between standard teacher and SFTN is 1.58% points, and the average difference between best student accuracy of standard teacher and SFTN is 1.10% points. We note that the outstanding performance of SFTN is not only driven by the higher accuracy of teacher models achieved by our student-aware learning technique. As observed in Table 1 and 2, the proposed approach often demonstrates substantial improvement compared to the standard distillation methods despite similar or lower teacher accuracies. Refer to Section 4.4 for the further discussion about the relation of teacher-student accuracy. Figure 3 illustrates the accuracies of the best student models of the standard teacher and SFTN given teacher and student architecture pairs. Despite the small capacity of the students, the best student models of SFTN sometimes outperform the standard teachers while the only one best student of the standard teacher shows higher accuracy than its teacher.

4.2.2. IMAGENET

ImageNet (Russakovsky et al., 2015) consists of 1.2M training images and 50K validation images for 1K classes. We adopt the standard Pytorch ImageNet training setup² for this experiment. The optimization is given by SGD with learning rate 0.1, weight decay 0.0001 and momentum 0.9. The coefficients of individual loss terms are set as $\lambda_T = 1$, $\lambda_R^{CE} = 1$, $\lambda_R^{KL} = 1$ and $\tau = 1$. We conduct the ImageNet experiment for 5 different knowledge distillation methods, where teacher models based on ResNet50 distill knowledge

Table 3. Top-1 and Top-5 validation accuracy on ImageNet.

Models (Teacher/Student)	ResNet50/ResNet34					
	Stan.	Top-1 SFTN	Δ	Stan.	Top-5 SFTN	Δ
Teacher training						
Teacher Acc.	76.45	77.43		93.15	93.75	
Stu. Acc. w/o KD		73.79			91.74	
KD	73.55	74.14	+0.59	91.81	92.21	+0.40
FitNets	74.56	75.01	+0.45	92.31	92.51	+0.20
SP	74.95	75.53	+0.58	92.54	92.69	+0.15
CRD	75.01	75.39	+0.38	92.56	92.67	+0.11
OH	74.56	75.01	+0.45	92.36	92.56	+0.20
Best	75.01	75.53	+0.52	92.56	92.69	+0.13

to ResNet34 student networks.

As presented in Table 3, SFTN consistently outperforms the standard teacher network in all settings. Also, the best student accuracy of SFTN achieves higher top-1 accuracy than standard teacher model by approximately 0.5% points. This results implies that the proposed SFTN has great potential on large datasets as well.

4.3. Comparison with Collaborative and Curriculum Learning Methods

Contrary to traditional knowledge distillation methods based on static pretrained teachers, collaborative learning and curriculum learning employ dynamic teacher networks trained with students jointly and the optimization history of teachers, respectively. Table 4 shows that SFTN outperforms the collaborative learning approaches such as DML (Zhang et al., 2018b) and KDCL (Guo et al., 2020); the heterogeneous architectures may not be effective for mutual learning. On the other hand, the accuracy of SFTN is consistently higher than that of the curriculum learning method, RCO (Jin et al., 2019) under the same and even harsher training condition in terms of epoch numbers; the identification of the optimal checkpoints may be challenging in trajectory-based learning. Note that SFTN improves its accuracy substantially with more iterations as shown in the results for SFTN-4.

4.4. Effect of Hyperparameters

SFTN computes the KL-divergence loss to minimize the difference between the softmax outputs of teacher and student branches, which involves two hyperparameters, temperature of the softmax function, τ , and weight for KL-divergence loss term, λ_R^{KL} . This subsection discusses the impact and trade-off issue of the two hyperparameters. In particular, we present our observations that the student-aware learning is indeed helpful to improve the accuracy of student models while maximizing performance of teacher models may be suboptimal for knowledge distillation.

Temperature of softmax function The temperature parameter, denoted by τ , controls the softness of \mathbf{q}_T and \mathbf{q}_R^i ;

¹<https://github.com/HobbitLong/RepDistille>

²<https://github.com/pytorch/examples/tree/master/imagenet>

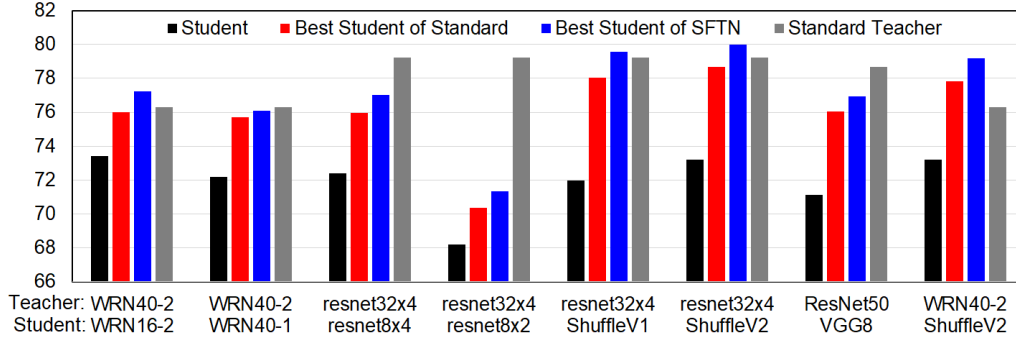


Figure 3. Accuracy comparison of the best students from SFTN with the standard teacher on CIFAR-100. The four best student models of SFTN outperform the standard teachers while the only one best student of the standard teacher shows higher accuracy than its teacher.

Table 4. Comparison with collaborative learning and curriculum learning approaches on CIFAR-100. We employ KDCL-Naïve for ensemble logits of KDCL. One stage EEI (equal epoch interval) and EEI-4 are adopted for training RCO. Both RCO-EEI-4 and SFTN-4 are trained for 240×4 epochs.

Teacher	WRN40-2		WRN40-2		resnet32x4		resnet32x4		resnet32x4		ResNet50	
Student	WRN16-2		WRN40-1		resnet8x4		ShuffleV1		ShuffleV2		VGG8	
Standard teacher Acc	76.3		76.3		79.25		79.25		79.25		78.7	
Student Acc. w/o KD	73.41		72.16		72.38		71.95		73.21		71.12	
	Student	Δ	Student	Δ	Student	Δ	Student	Δ	Student	Δ	Student	Δ
Standard	75.46	+2.05	73.73	+1.57	73.39	+1.01	74.26	+2.31	75.25	+2.04	73.82	+2.7
DML	75.30	+1.89	74.08	+1.92	74.34	+1.96	73.37	+1.42	73.80	+0.59	73.01	+1.89
KDCL	75.45	+2.04	74.65	+2.49	75.21	+2.83	73.98	+2.03	74.30	+1.09	73.48	+2.36
RCO-one-stage-EEI	75.36	+1.95	74.29	+2.13	74.06	+1.68	76.62	+4.67	77.40	+4.19	74.30	+3.18
SFTN	76.25	+2.84	75.09	+2.93	76.09	+3.71	77.93	+5.98	78.07	+4.86	74.92	+3.80
RCO-EEI-4	75.69	+2.28	74.87	+2.71	73.73	+1.35	76.97	+5.02	76.89	+3.68	74.24	+3.12
SFTN-4	76.96	+3.55	76.31	+4.15	76.67	+4.29	79.11	+7.16	78.95	+5.74	75.52	+4.40

Table 5. Effects of varying τ in the knowledge distillation via SFTN. The student accuracy is fairly stable over a wide range of the parameter. Note that the accuracies of SFTN and student are rather inversely correlated, which implies that the maximization of teacher models is not necessarily idea for knowledge distillation.

Teacher	Accuracy of SFTN					Student accuracy by KD				
	resnet32x4	resnet32x4	WRN40-2	WRN40-2	AVG	resnet32x4	resnet32x4	WRN40-2	WRN40-2	AVG
Student	ShuffleV1	ShuffleV2	WRN16-2	WRN40-1		ShuffleV1	ShuffleV2	WRN16-2	WRN40-1	
$\tau=1$	81.19	80.26	78.23	78.14	78.85	76.05	77.18	76.30	74.75	75.58
$\tau=5$	81.23	81.56	79.22	78.31	79.54	75.36	75.59	76.31	73.64	75.10
$\tau=10$	81.27	81.98	78.81	78.38	79.58	74.47	75.93	75.85	73.62	74.76
$\tau=15$	81.89	81.74	79.27	78.63	79.74	74.78	75.65	75.79	73.49	74.81
$\tau=20$	81.60	81.70	78.84	78.45	79.59	74.62	75.88	75.82	74.03	74.95

Table 6. Effects of varying λ_R^{KL} in the knowledge distillation via SFTN. The accuracies of SFTN and student are not correlated while the accuracy gaps of the two model drops as λ_R^{KL} increases.

Teacher	Accuracy of SFTN					Student accuracy by KD				
	resnet32x4	resnet32x4	WRN40-2	WRN40-2	AVG	resnet32x4	resnet32x4	WRN40-2	WRN40-2	AVG
Student	ShuffleV1	ShuffleV2	WRN16-2	WRN40-1		ShuffleV1	ShuffleV2	WRN16-2	WRN40-1	
$\lambda_R^{KL}=1$	81.19	80.26	78.23	78.14	79.46	76.05	77.18	76.30	74.75	76.07
$\lambda_R^{KL}=3$	78.70	79.80	77.83	77.57	78.48	77.36	78.56	76.20	74.71	76.71
$\lambda_R^{KL}=6$	78.29	78.29	77.28	76.05	77.48	77.33	77.70	76.02	74.67	76.43
$\lambda_R^{KL}=10$	73.02	75.01	75.03	73.51	74.14	75.57	76.62	74.19	73.08	74.87
Standard	79.25	79.25	76.30	76.30	77.78	74.31	75.25	75.28	73.56	74.60

as τ gets higher, the output of the softmax function becomes smoother. Despite the fluctuation in teacher accuracy, student models given by KD via SFTN maintain fairly consistent results. Table 5 also shows that the performance of

SFTNs and student models is rather inversely correlated. In other words, a loosely optimized teacher model turns out to be more effective for knowledge distillation according to this ablation study.

Table 7. The accuracy of student models on STL10 and TinyImageNet by transferring knowledge from the models trained on CIFAR-100.

Models (Teacher/Student)	resnet32x4/ShuffleV2					
	CIFAR100 → STL10			CIFAR100 → TinyImageNet		
Teacher training method	Standard	SFTN	Δ	Standard	SFTN	Δ
Teacher accuracy	69.81	76.84		31.25	40.16	
Student accuracy w/o KD		70.18			33.81	
KD	67.49	73.81	+6.32	30.45	37.81	+7.36
SP	69.56	75.01	+5.45	31.16	38.28	+7.12
CRD	71.70	75.80	+4.10	35.50	40.87	+5.37
SSKD	74.43	77.45	+3.02	38.35	42.41	+4.06
OH	72.09	76.76	+4.67	33.52	39.95	+6.43
AVG	71.05	75.77	+4.71	33.80	39.86	+6.07

Weight for KL-divergence loss λ_R^{KL} is a parameter that makes \mathbf{q}_T similar to \mathbf{q}_R^i , and consequently facilitates knowledge distillation. However, it affects the accuracy of teacher network negatively. Table 6 shows that the average accuracy gaps between SFTNs and student models drops gradually as λ_R^{KL} increases. One interesting observation is the student accuracy via SFTN with $\lambda_R^{KL} = 10$ compared to its counterpart via the standard teacher; even though the standard teacher network is more accurate than SFTN by a large margin, its corresponding student accuracy is lower than that of SFTN.

4.5. Transferability

The goal of transfer learning is to obtain versatile representations that adapt well on unseen datasets. To investigate transferability of the student models distilled from SFTN, we perform experiments to transfer the student features learned on CIFAR-100 to STL10 (Coates et al., 2011) and TinyImageNet (<http://tinyimagenet.herokuapp.com/>). The representations of the examples in CIFAR-100 are obtained from the last student block and frozen during transfer learning, and then we make the features fit to the target datasets using linear classifiers attached to the last student block.

Table 7 presents transfer learning results on 5 different knowledge distillation algorithms using ResNet32×4 and ShuffleV2 as teacher and student, respectively. Our experiments show that the accuracy of transfer learning on the student models derived from SFTN is consistently better than the students associated with the standard teacher. The average student accuracy of SFTN even outperforms that of the standard teacher by 4.71% points on STL10 and 6.07% points on TinyImageNet.

4.6. Similarity

Similarity between student and teacher network is an important measure for knowledge distillation tasks considering student network is basically trying to resemble similar output of teacher network. We employ KL-divergence and CKA (Kornblith et al., 2019) as metrics of similarity between student and teacher network, where lower KL-divergence and higher CKA imply higher similarity. Table 8

Table 8. Similarity measurements between teachers and students on the CIFAR-100 test set. Higher CKA and lower KL indicate that the representations given by two models are more similar.

Models (Teacher/Student)	resnet32x4/ShuffleV2			
	KL-divergence		CKA	
Teacher training method	Standard	SFTN	Standard	SFTN
KD	1.10	0.47	0.88	0.95
FitNets	0.79	0.38	0.89	0.95
SP	0.95	0.45	0.89	0.95
VID	0.88	0.45	0.88	0.95
CRD	0.81	0.43	0.88	0.95
SSKD	0.54	0.26	0.92	0.97
OH	0.85	0.37	0.90	0.96
AVG	0.84	0.39	0.89	0.96

presents the similarities between the representations of a ResNet32×4 teacher and a ShuffleV2 student given by various algorithms on the CIFAR-100 test set. The results show that the distillation from SFTN always gives higher similarity to the student model with respect to the teacher network; SFTN reduces KL-divergence by 50% in average while improving average CKA by 7% points compared to the standard teacher network. Since SFTN is trained with student branches to obtain student-friendly representations via a KL-divergence loss, the improved similarity is natural.

5. Conclusion

We proposed a simple but effective knowledge distillation approach by introducing the novel student-friendly teacher network (SFTN). Our strategy sheds a light in a new direction to knowledge distillation, which focus on the stage to train teacher networks. We train teacher networks along with their student branches, and then perform distillation from teachers to students. The proposed strategy turns out to improve training efficiency greatly, and can be incorporated into various knowledge distillation algorithms in a straightforward manner. For the demonstration of the effectiveness of our strategy, we conducted comprehensive experiments in diverse environments, which show consistent performance gains compared to the standard teacher networks regardless of architectural and algorithmic variations.

References

- Ahn, S., Hu, S. X., Damianou, A. C., Lawrence, N. D., and Dai, Z. Variational information distillation for knowledge transfer. In *CVPR*, 2019.
- Arora, S., Khapra, M. M., and Ramaswamy, H. G. On knowledge distillation from complex networks for response prediction. In Burstein, J., Doran, C., and Solorio, T. (eds.), *NAACL*, 2019.
- Chen, G., Choi, W., Chen, X., Han, T. X., and Chandraker, M. K. Learning Efficient Object Detection Models with Knowledge Distillation. In *NeurIPS*, 2017.
- Cho, J. H. and Hariharan, B. On the efficacy of knowledge distillation. In *ICCV*, 2019.
- Coates, A., Ng, A. Y., and Lee, H. An analysis of single-layer networks in unsupervised feature learning. In *AISTATS*, 2011.
- Furlanello, T., Lipton, Z. C., Tschannen, M., Itti, L., and Anandkumar, A. Born-again neural networks. In *ICML*, 2018.
- Guo, Q., Wang, X., Wu, Y., Yu, Z., Liang, D., Hu, X., and Luo, P. Online knowledge distillation via collaborative learning. In *CVPR*, 2020.
- He, K., Zhang, X., Ren, S., and Sun, J. Deep Residual Learning for Image Recognition. In *CVPR*, 2016.
- Heo, B., Kim, J., Yun, S., Park, H., Kwak, N., and Choi, J. Y. A comprehensive overhaul of feature distillation. In *ICCV*, 2019a.
- Heo, B., Lee, M., Yun, S., and Choi, J. Y. Knowledge transfer via distillation of activation boundaries formed by hidden neurons. In *AAAI*, 2019b.
- Hinton, G., Vinyals, O., and Dean, J. Distilling the Knowledge in a Neural Network. In *NeurIPS Deep Learning and Representation Learning Workshop*, 2015.
- <http://tiny-imagenet.herokuapp.com/>.
- Jiao, X., Yin, Y., Shang, L., Jiang, X., Chen, X., Li, L., Wang, F., and Liu, Q. Tinybert: Distilling BERT for natural language understanding. *CoRR*, 2019.
- Jin, X., Peng, B., Wu, Y., Liu, Y., Liu, J., Liang, D., Yan, J., and Hu, X. Knowledge distillation via route constrained optimization. In *ICCV*, 2019.
- Kang, M., Mun, J., and Han, B. Towards oracle knowledge distillation with neural architecture search. In *AAAI*, 2020.
- Kim, J., Park, S., and Kwak, N. Paraphrasing Complex Network: Network Compression via Factor Transfer. In *NeurIPS*, 2018.
- Kornblith, S., Norouzi, M., Lee, H., and Hinton, G. E. Similarity of neural network representations revisited. In *ICML*, 2019.
- Krizhevsky, A. Learning Multiple Layers of Features from Tiny Images. Technical report, Citeseer, 2009.
- lan, x., Zhu, X., and Gong, S. Knowledge Distillation by On-the-Fly Native Ensemble. In *NeurIPS*, 2018.
- Luo, P., Zhu, Z., Liu, Z., Wang, X., and Tang, X. Face Model Compression by Distilling Knowledge from Neurons. In *AAAI*, 2016.
- Mirzadeh, S.-I., Farajtabar, M., Li, A., and Ghasemzadeh, H. Improved knowledge distillation via teacher assistant: Bridging the gap between student and teacher. In *AAAI*, 2020.
- Mun, J., Lee, K., Shin, J., and Han, B. Learning to Specialize with Knowledge Distillation for Visual Question Answering. In *NeurIPS*, 2018.
- Park, W., Kim, D., Lu, Y., and Cho, M. Relational Knowledge Distillation. In *CVPR*, 2019.
- Passalis, N. and Tefas, A. Learning deep representations with probabilistic knowledge transfer. In *ECCV*, 2018.
- Romero, A., Ballas, N., Kahou, S. E., Chassang, A., Gatta, C., and Bengio, Y. FitNets: Hints for Thin Deep Nets. In *ICLR*, 2015.
- Russakovsky, O., Deng, J., Su, H., Krause, J., Satheesh, S., Ma, S., Huang, Z., Karpathy, A., Khosla, A., Bernstein, M. S., Berg, A. C., and Li, F. Imagenet large scale visual recognition challenge. *Int. J. Comput. Vis.*, 115(3):211–252, 2015.
- Sanh, V., Debut, L., Chaumond, J., and Wolf, T. Distilbert, a distilled version of BERT: smaller, faster, cheaper and lighter. *CoRR*, 2019.
- Simonyan, K. and Zisserman, A. Very Deep Convolutional Networks for Large-Scale Image Recognition. In *ICLR*, 2015.
- Tan, M., Chen, B., Pang, R., Vasudevan, V., Sandler, M., Howard, A., and Le, Q. V. Mnasnet: Platform-aware neural architecture search for mobile. In *CVPR*, 2019.
- Thoker, F. M. and Gall, J. Cross-modal knowledge distillation for action recognition. In *ICIP*, 2019.
- Tian, Y., Krishnan, D., and Isola, P. Contrastive representation distillation. In *ICLR*, 2020.

- Tung, F. and Mori, G. Similarity-preserving knowledge distillation. In *ICCV*, 2019.
- Wang, H., Li, Y., Wang, Y., Hu, H., and Yang, M. Collaborative distillation for ultra-resolution universal style transfer. In *CVPR*, 2020.
- Wu, A., Zheng, W., Guo, X., and Lai, J. Distilled person re-identification: Towards a more scalable system. In *CVPR*, 2019.
- Wu, G. and Gong, S. Peer collaborative learning for online knowledge distillation. In *arXiv 2006.04147*, 2020.
- Xu, G., Liu, Z., Li, X., and Loy, C. C. Knowledge distillation meets self-supervision. In *ECCV*, 2020.
- Zagoruyko, S. and Komodakis, N. Wide residual networks. In *BMVC*, 2016.
- Zagoruyko, S. and Komodakis, N. Paying More Attention to Attention: Improving the Performance of Convolutional Neural Networks via Attention Transfer. In *ICLR*, 2017.
- Zhang, L., Song, J., Gao, A., Chen, J., Bao, C., and Ma, K. Be your own teacher: Improve the performance of convolutional neural networks via self distillation. In *ICCV*, 2019.
- Zhang, X., Zhou, X., Lin, M., and Sun, J. Shufflenet: An extremely efficient convolutional neural network for mobile devices. In *CVPR*, 2018a.
- Zhang, Y., Xiang, T., Hospedales, T. M., and Lu, H. Deep Mutual Learning. In *CVPR*, 2018b.
- Zhao, M., Li, T., Alsheikh, M. A., Tian, Y., Zhao, H., Torralba, A., and Katabi, D. Through-wall human pose estimation using radio signals. In *CVPR*, 2018.
- Zhou, B., Kalra, N., and Krähenbühl, P. Domain adaptation through task distillation. In *ECCV*, 2020.

Learning Student-Friendly Teacher Networks for Knowledge Distillation

Supplementary Document

6. More Analysis

6.1. Effectiveness of Training Student-Aware Teacher Networks

For training a student-aware teacher network, the proposed approach adopts the student branch whose structure matches with the student network for knowledge distillation. To analyze the effectiveness of student-aware teacher networks, we present how the size of the student branch affects the performances of SFTN when the student model is fixed. Table 9 shows that the student branches with the identical structures to the target student networks achieve the best accuracy in general. Note that larger students branches are often effective to enhance the accuracy of teachers and the smaller ones tend to lose their accuracy.

6.2. Relationship between Teacher and Student Accuracies

Figure 4 illustrates the relationship between teacher and student accuracies. According to our experiment, higher teacher accuracy does not necessarily lead to better student models. Also, even in the case that the teacher accuracies of SFTN are lower than those of the standard method, the student models of SFTN consistently outperform the counterparts of the standard method. This result implies that the performance improvement of teacher models is not the main reason for the better results of SFTN.

6.3. Training and Testing Curves

Figure 5(a) illustrates the KL-divergence loss of SFTN for knowledge distillation converges faster than the standard teacher network. This would be because, by the student-aware training through student branches, SFTN learns better transferrable knowledge to student model than the standard teacher network. We believe that it leads to higher test accuracies of SFTN as shown in Figure 5(b).

7. Implementation Details

We present the details of our implementation for better reproduction.

7.1. CIFAR-100

The models for CIFAR-100 are trained for 240 epochs with a batch size of 64, where the learning rate is reduced by a factor of 10 at the 150th, 180th, and 210th epochs. We use randomly cropped 32×32 image with 4 pixel padded and adopt horizontal flipping with a probability of 0.5 for data augmentation. Each channel in an input image is normalized to the standard Gaussian.

7.2. ImageNet

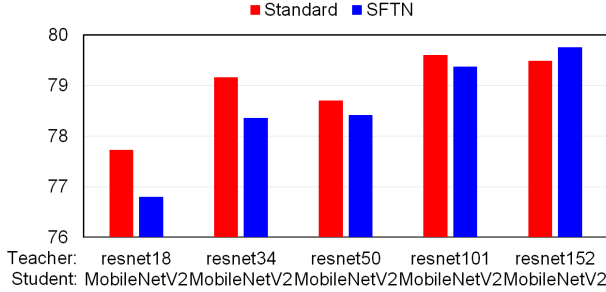
ImageNet models are learned for 100 epochs with a batch size of 256. We reduce the learning rate by an order of magnitude at the 30th, 60th, and 90th epochs. In training phase, we perform random cropping with the range from 0.08 to 1.0, which denotes the relative size to the original image while the aspect ratios are adjusted randomly by multiplying a scalar value between 3/4 and 4/3 to the original aspect. All images are resized to 224×224 and flipped horizontally with a probability of 0.5. In validation phase, images are resized to 256×256 , and then center-cropped to 224×224 . Each channel in an input image is normalized to the standard Gaussian.

8. Architecture Details

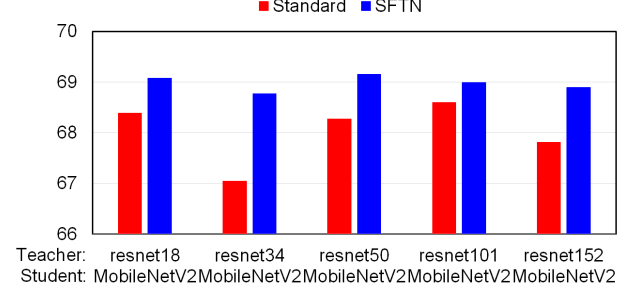
We present the architectural details of SFTN with VGG13 and VGG8 respectively for teacher and student on CIFAR100. VGG13 and VGG8 are modularized into 4 blocks based on the depths of layers and the feature map sizes. VGG13 SFTN adds a student branch to every output of the teacher network block except the last teacher network block. Figure 6, 7 and 8 show the architectures of VGG13 teacher, VGG8 student and VGG13 SFTN with a VGG8 student branch attached. Table 10, 11 and 12 describe the full details of the architectures.

Table 9. Effectiveness of training student-aware teacher networks before knowledge distillation. For each teacher and student branch pairs adopted in the student-aware teacher network training stage, we evaluate knowledge distillation performance of three different student branch sizes. The results show that matching model architectures between the two stages—student-aware teacher network training and knowledge distillation—leads to the best accuracies in general, which implies the practical benefit of SFTN. Note that all the results numbers are given by the averages of 3 independent runs. Bold-faced numbers indicate the highest accuracies among the various student branch models.

Models (teacher/student)	WRN40-2/resnet8x4			resnet32x4/resnet8x4			resnet32x4/WRN16-2		
Student branch size	Smaller	Equal	Larger	Smaller	Equal	Larger	Smaller	Equal	Larger
Student branch model	resnet8x2	resnet8x4	resnet32x4	resnet8x2	resnet8x4	resnet32x4	WRN16-1	WRN16-2	WRN40-2
Teacher accuracy	76.22	78.18	78.82	77.89	79.41	80.85	76.53	79.04	80.3
Student Acc. w/o KD		72.38			71.12			73.41	
KD	74.08	75.46	74.84	75.19	76.09	75.19	75.14	76.33	76.37
SP	74.01	75.58	75.24	75.76	76.37	75.62	75.61	76.91	76.34
FT	74.55	75.83	76.03	76.54	77.02	76.48	76.26	77.07	76.81
CRD	75.8	76.94	76.52	76.72	76.95	76.54	76.55	77.39	77.27
SSKD	73.67	75.85	75.93	75.77	76.85	76.67	75.27	77.14	77.35
OH	74.79	75.98	76.09	75.69	76.65	76.38	75.85	76.87	77.00
Average	74.48	75.94	75.78	75.94	76.66	76.15	75.78	76.95	76.86
Best	75.8	76.94	76.52	76.72	77.02	76.67	76.55	77.39	77.35

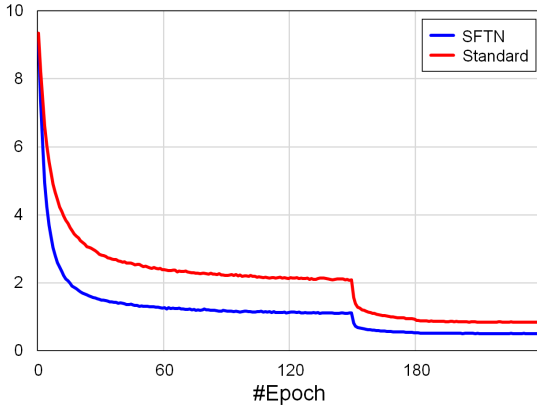


(a) Teacher accuracy on CIFAR-100.

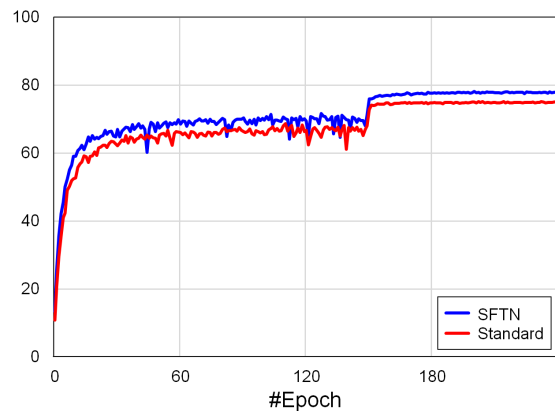


(b) Student Accuracy by KD.

Figure 4. Relationship between teacher and student accuracies tested on CIFAR-100, where resnet with different sizes and MobileNetV2 are employed as teacher and student networks, respectively. Generally, the teacher accuracy of SFTN is lower than the standard teacher network, but the student models of SFTN is consistently outperform standard methods.



(a) KL-divergence loss during training on CIFAR-100.



(b) Test accuracy on CIFAR-100.

Figure 5. Visualization of training and testing curves on CIFAR-100, where resnet32 \times 4 and ShuffleV2 are employed as teacher and student networks, respectively. SFTN converges faster and show improved test accuracy than the standard teacher models.

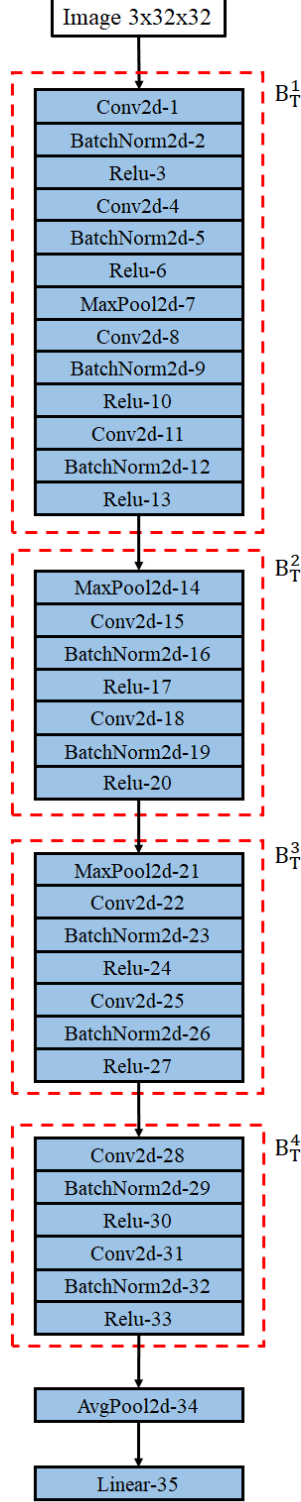


Figure 6. Architecture of VGG13 teacher model. B_T^i and B_S^i denote the i^{th} block of teacher network and the i^{th} block of student network, respectively. Table 10 shows detailed description of VGG13 teacher.

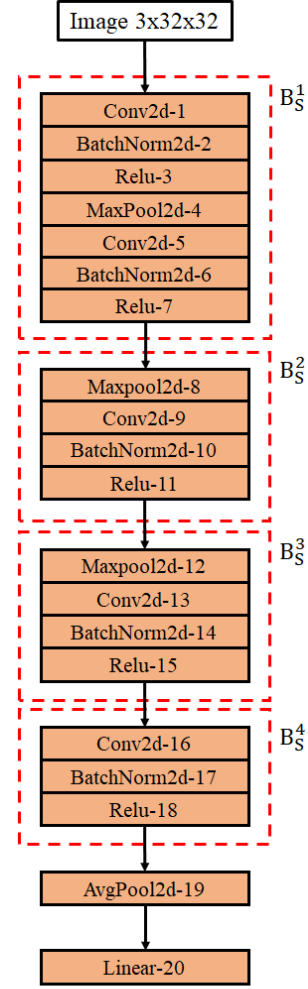


Figure 7. Architecture of VGG8 student. B_T^i and B_S^i denote the i^{th} block of teacher network and the i^{th} block of student network, respectively. Table 11 shows detailed description of VGG8 student.

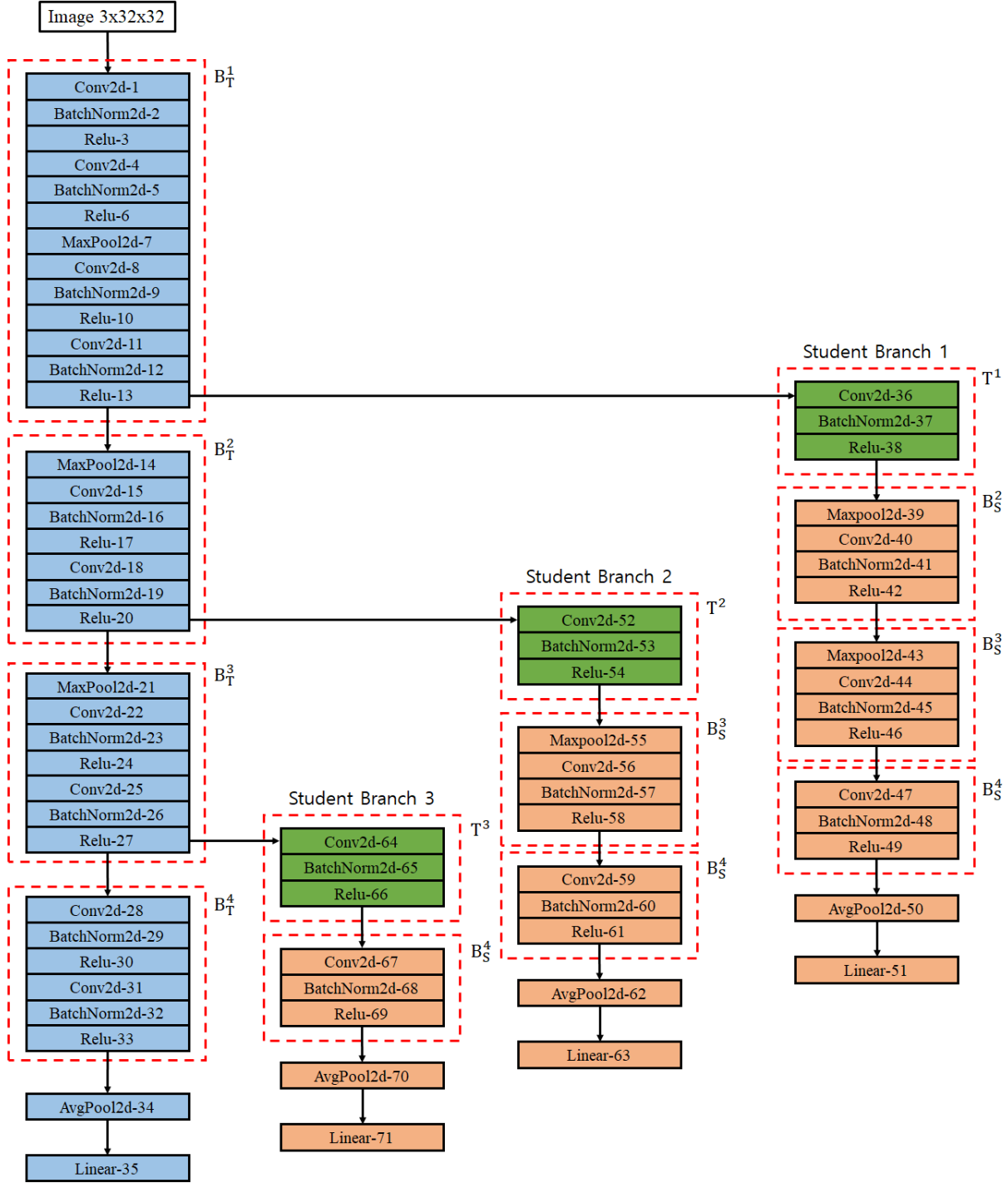


Figure 8. Architecture of SFTN with VGG13 teacher and VGG8 student branch. B_T^i , B_S^i and T^i denote the i^{th} block of teacher network, the i^{th} block of student network and teacher network feature transform layer, respectively. Table 12 shows detailed description of VGG13 SFTN attached VGG8 student branch.

Table 10. VGG13 detailed teacher.

Layer	Input Layer	Input Shape	Filter Size	Channels	Stride	Paddings	Output Shape	Block
Image	-	-	-	-	-	-	3x32x32	-
Conv2d-1	Image	3x32x32	3x3	64	1	1	64x32x32	B_T^1
BatchNorm2d-2	Conv2d-1	64x32x32	-	64	-	-	64x32x32	
Relu-3	BatchNorm2d-2	64x32x32	-	-	-	-	64x32x32	
Conv2d-4	Relu-3	64x32x32	3x3	64	1	1	64x32x32	
BatchNorm2d-5	Conv2d-4	64x32x32	-	64	-	-	64x32x32	
Relu-6	BatchNorm2d-5	64x32x32	-	-	-	-	64x32x32	
MaxPool2d-7	Relu-6	64x32x32	2x2	-	2	0	64x16x16	
Conv2d-8	MaxPool2d-7	64x16x16	3x3	128	1	1	128x16x16	
BatchNorm2d-9	Conv2d-8	128x16x16	-	128	-	-	128x16x16	
Relu-10	BatchNorm2d-9	128x16x16	-	-	-	-	128x16x16	
Conv2d-11	Relu-10	128x16x16	3x3	128	1	1	128x16x16	
BatchNorm2d-12	Conv2d-11	128x16x16	-	128	-	-	128x16x16	
Relu-13	BatchNorm2d-12	128x16x16	-	-	-	-	128x16x16	
MaxPool2d-14	Relu-13	128x16x16	2x2	-	2	0	128x8x8	B_T^2
Conv2d-15	MaxPool2d-14	128x8x8	3x3	256	1	1	256x8x8	
BatchNorm2d-16	Conv2d-15	256x8x8	-	256	-	-	256x8x8	
Relu-17	BatchNorm2d-16	256x8x8	-	-	-	-	256x8x8	
Conv2d-18	Relu-17	256x8x8	3x3	256	1	1	256x8x8	
BatchNorm2d-19	Conv2d-18	256x8x8	-	256	-	-	256x8x8	
Relu-20	BatchNorm2d-19	256x8x8	-	-	-	-	256x8x8	B_T^3
MaxPool2d-21	Relu-20	256x8x8	2x2	-	2	0	256x4x4	
Conv2d-22	MaxPool2d-21	256x4x4	3x3	512	1	1	512x4x4	
BatchNorm2d-23	Conv2d-22	512x4x4	-	512	-	-	512x4x4	
Relu-24	BatchNorm2d-23	512x4x4	-	-	-	-	512x4x4	
Conv2d-25	Relu-24	512x4x4	3x3	512	1	1	512x4x4	
BatchNorm2d-26	Conv2d-25	512x4x4	-	512	-	-	512x4x4	B_T^4
Relu-27	BatchNorm2d-26	512x4x4	-	-	-	-	512x4x4	
Conv2d-28	Relu-27	512x4x4	3x3	512	1	1	512x4x4	
BatchNorm2d-29	Conv2d-28	512x4x4	-	512	-	-	512x4x4	
Relu-30	BatchNorm2d-29	512x4x4	-	-	-	-	512x4x4	
Conv2d-31	Relu-30	512x4x4	3x3	512	1	1	512x4x4	
BatchNorm2d-32	Conv2d-31	512x4x4	-	512	-	-	512x4x4	-
Relu-33	BatchNorm2d-32	512x4x4	-	-	-	-	512x4x4	
AvgPool2d-34	Relu-33	512x4x4	-	-	-	-	512x1x1	-
Linear-35	AvgPool2d-34	512x1x1	-	-	-	-	100	-

Table 11. VGG8 student model.

Layer	Input Layer	Input Shape	Filter Size	Channels	Stride	Paddings	Output Shape	Block
Image	-	-	-	-	-	-	3x32x32	-
Conv2d-1	Image	3x32x32	3x3	64	1	1	64x32x32	B_S^1
BatchNorm2d-2	Conv2d-1	64x32x32	-	64	-	-	64x32x32	
Relu-3	BatchNorm2d-2	64x32x32	-	-	-	-	64x32x32	
MaxPool2d-4	Relu-3	64x32x32	2x2	-	2	0	64x16x16	
Conv2d-5	MaxPool2d-4	64x16x16	3x3	128	1	1	128x16x16	
BatchNorm2d-6	Conv2d-5	128x16x16	2x2	128	1	-	128x16x16	
Relu-7	BatchNorm2d-6	128x16x16	-	-	-	-	128x16x16	
Maxpool2d-8	Relu-7	128x16x16	2x2	-	2	0	128x8x8	B_S^2
Conv2d-9	Maxpool2d-8	128x8x8	3x3	256	1	1	256x8x8	
BatchNorm2d-10	Conv2d-9	256x8x8	-	256	-	-	256x8x8	
Relu-11	BatchNorm2d-10	256x8x8	-	-	-	-	256x8x8	
MaxPool2d-12	Relu-11	256x8x8	2x2	-	2	0	256x4x4	B_S^3
Conv2d-13	MaxPool2d-12	256x4x4	3x3	512	1	1	512x4x4	
BatchNorm2d-14	Conv2d-13	512x4x4	-	512	-	-	512x4x4	
Relu-15	BatchNorm2d-14	512x4x4	-	-	-	-	512x4x4	
Conv2d-16	Relu-15	512x4x4	3x3	512	1	1	512x4x4	B_S^4
BatchNorm2d-17	Conv2d-16	512x4x4	-	512	-	-	512x4x4	
Relu-18	BatchNorm2d-17	512x4x4	-	-	-	-	512x4x4	
AvgPool2d-19	Relu-18	512x4x4	-	-	-	-	512x1x1	-
Linear-20	AvgPool2d-19	512x1x1	-	-	-	-	100	-

Table 12. Details of SFTN architecture with VGG13 teacher and VGG8 student branch.

Layer	Input Layer	Input Shape	Filter Size	Channels	Stride	Paddings	Output Shape	Block
Image	-	-	-	-	-	-	3x32x32	-
Conv2d-1	Image	3x32x32	3x3	64	1	1	64x32x32	B_T^1
BatchNorm2d-2	Conv2d-1	64x32x32	-	64	-	-	64x32x32	
Relu-3	BatchNorm2d-2	64x32x32	-	-	-	-	64x32x32	
Conv2d-4	Relu-3	64x32x32	3x3	64	1	1	64x32x32	
BatchNorm2d-5	Conv2d-4	64x32x32	-	64	-	-	64x32x32	
Relu-6	BatchNorm2d-5	64x32x32	-	-	-	-	64x32x32	
MaxPool2d-7	Relu-6	64x32x32	2x2	-	2	0	64x16x16	
Conv2d-8	MaxPool2d-7	64x16x16	3x3	128	1	1	128x16x16	
BatchNorm2d-9	Conv2d-8	128x16x16	-	128	-	-	128x16x16	
Relu-10	BatchNorm2d-9	128x16x16	-	-	-	-	128x16x16	
Conv2d-11	Relu-10	128x16x16	3x3	128	1	1	128x16x16	
BatchNorm2d-12	Conv2d-11	128x16x16	-	128	-	-	128x16x16	
Relu-13	BatchNorm2d-12	128x16x16	-	-	-	-	128x16x16	
MaxPool2d-14	Relu-13	128x16x16	2x2	-	2	0	128x8x8	B_T^2
Conv2d-15	MaxPool2d-14	128x8x8	3x3	256	1	1	256x8x8	
BatchNorm2d-16	Conv2d-15	256x8x8	-	256	-	-	256x8x8	
Relu-17	BatchNorm2d-16	256x8x8	-	-	-	-	256x8x8	
Conv2d-18	Relu-17	256x8x8	3x3	256	1	1	256x8x8	
BatchNorm2d-19	Conv2d-18	256x8x8	-	256	-	-	256x8x8	
Relu-20	BatchNorm2d-19	256x8x8	-	-	-	-	256x8x8	B_T^3
MaxPool2d-21	Relu-20	256x8x8	2x2	-	2	0	256x4x4	
Conv2d-22	MaxPool2d-21	256x4x4	3x3	512	1	1	512x4x4	
BatchNorm2d-23	Conv2d-22	512x4x4	-	512	-	-	512x4x4	
Relu-24	BatchNorm2d-23	512x4x4	-	-	-	-	512x4x4	
Conv2d-25	Relu-24	512x4x4	3x3	512	1	1	512x4x4	
BatchNorm2d-26	Conv2d-25	512x4x4	-	512	-	-	512x4x4	B_T^4
Relu-27	BatchNorm2d-26	512x4x4	-	-	-	-	512x4x4	
Conv2d-28	Relu-27	512x4x4	3x3	512	1	1	512x4x4	
BatchNorm2d-29	Conv2d-28	512x4x4	-	512	-	-	512x4x4	
Relu-30	BatchNorm2d-29	512x4x4	-	-	-	-	512x4x4	
Conv2d-31	Relu-30	512x4x4	3x3	512	1	1	512x4x4	
BatchNorm2d-32	Conv2d-31	512x4x4	-	512	-	-	512x4x4	-
Relu-33	BatchNorm2d-32	512x4x4	-	-	-	-	512x4x4	
AvgPool2d-34	Relu-33	512x4x4	-	-	-	-	512x1x1	-
Linear-35	AvgPool2d-34	512x1x1	-	-	-	-	100	-
Student Branch 1								
Conv2d-36	Relu-13	128x16x16	1x1	128	1	0	128x16x16	\mathcal{T}^1
BatchNorm2d-37	Conv2d-36	128x16x16	-	128	-	-	128x16x16	
Relu-38	BatchNorm2d-37	128x16x16	-	-	-	-	128x16x16	
Maxpool2d-39	BatchNorm2d-37	128x16x16	2x2	-	2	0	128x8x8	B_S^2
Conv2d-40	Maxpool2d-39	128x8x8	3x3	256	1	1	256x8x8	
BatchNorm2d-41	Conv2d-40	256x8x8	-	256	-	-	256x8x8	
Relu-42	BatchNorm2d-41	-	-	-	-	-	256x8x8	B_S^3
MaxPool2d-43	Relu-42	256x8x8	2x2	-	2	0	256x4x4	
Conv2d-44	MaxPool2d-43	256x4x4	3x3	512	1	1	512x4x4	
BatchNorm2d-45	Conv2d-44	512x4x4	-	512	-	-	512x4x4	
Relu-46	BatchNorm2d-45	-	-	-	-	-	512x4x4	B_S^4
Conv2d-47	Relu-46	512x4x4	3x3	512	1	1	512x4x4	
BatchNorm2d-48	Conv2d-47	512x4x4	-	512	-	-	512x4x4	
Relu-49	BatchNorm2d-48	-	-	-	-	-	512x4x4	-
AvgPool2d-50	Relu-49	512x4x4	-	-	-	-	512x1x1	
Linear-51	AvgPool2d-50	512x1x1	-	-	-	-	100	-

Table 3. Continued from the previous table.

Layer	Input Layer	Input Shape	Filter Size	Channels	Stride	Paddings	Output Shape	Block
Student Branch 2								
Conv2d-52	Relu-20	256x8x8	1x1	256	1	0	256x8x8	\mathcal{T}^2
BatchNorm2d-53	Conv2d-52	256x8x8	-	256	-	-	256x8x8	
Relu-54	BatchNorm2d-53	256x8x8	-	-	-	-	256x8x8	
MaxPool2d-55	Relu-54	256x8x8	2x2	-	2	0	256x4x4	B_S^3
Conv2d-56	MaxPool2d-55	256x4x4	3x3	512	1	1	512x4x4	
BatchNorm2d-57	Conv2d-56	512x4x4	-	512	-	-	512x4x4	
Relu-58	BatchNorm2d-57	-	-	-	-	-	512x4x4	
Conv2d-59	Relu-58	512x4x4	3x3	512	1	1	512x4x4	B_S^4
BatchNorm2d-60	Conv2d-59	512x4x4	-	512	-	-	512x4x4	
Relu-61	BatchNorm2d-60	-	-	-	-	-	512x4x4	
AvgPool2d-62	Relu-61	512x4x4	-	-	-	-	512x1x1	-
Linear-63	AvgPool2d-62	512x1x1	-	-	-	-	100	-
Student Branch 3								
Conv2d-64	Relu-27	512x4x4	1x1	512	1	0	512x4x4	\mathcal{T}^3
BatchNorm2d-65	Conv2d-64	512x4x4	-	512	-	-	512x4x4	
Relu-66	BatchNorm2d-65	512x4x4	-	-	-	-	512x4x4	
Conv2d-67	Relu-66	512x4x4	3x3	512	1	1	512x4x4	B_S^4
BatchNorm2d-68	Conv2d-67	512x4x4	-	512	-	-	512x4x4	
Relu-69	BatchNorm2d-68	-	-	-	-	-	512x4x4	
AvgPool2d-70	Relu-69	512x4x4	-	-	-	-	512x1x1	
Linear-71	AvgPool2d-70	512x1x1	-	-	-	-	100	-